

## Article

# Performance Estimation Modeling via Machine Learning of an Agrophotovoltaic System in South Korea

Sojung Kim <sup>1</sup>  and Sumin Kim <sup>2,\*</sup> <sup>1</sup> Industrial and Systems Engineering, Dongguk University-Seoul, Seoul 04620, Korea; sojungkim@dgu.ac.kr<sup>2</sup> Department of Environmental Horticulture & Landscape Architecture, College of Life Science & Biotechnology, Dankook University, Cheonan-si 31116, Korea

\* Correspondence: sumin.kim@dankook.ac.kr; Tel.: +82-41-550-3644

**Abstract:** The Agrophotovoltaic (APV) system is a novel concept in the field of Renewable Energy Systems. This system enables the generation of solar energy via photo-voltaic (PV) modules above crops, to mitigate harmful impact on food production. This study aims to develop a performance evaluation model for an APV system in a temperate climate region, such as South Korea. To this end, both traditional electricity generation models (solar radiation-based model and climate-based model) of PV modules and two major machine learning (ML) techniques (i.e., polynomial regression and deep learning) have been considered. Electricity generation data was collected via remote sensors installed in the APV system at Jeollanam-do Agricultural Research and Extension Services in South Korea. Moreover, economic analysis in terms of cost and benefit of the subject APV system was conducted to provide information about the return on investment to farmers and government agencies. As a result, farmers, agronomists, and agricultural engineers can easily estimate performance and profit of their APV systems via the proposed performance model.

**Keywords:** Agrophotovoltaic; photovoltaic; renewable energy; energy system; machine learning



**Citation:** Kim, S.; Kim, S. Performance Estimation Modeling via Machine Learning of an Agrophotovoltaic System in South Korea. *Energies* **2021**, *14*, 6724. <https://doi.org/10.3390/en14206724>

Academic Editor: Idiano D'Adamo

Received: 16 September 2021

Accepted: 13 October 2021

Published: 15 October 2021

**Publisher's Note:** MDPI stays neutral with regard to jurisdictional claims in published maps and institutional affiliations.



**Copyright:** © 2021 by the authors. Licensee MDPI, Basel, Switzerland. This article is an open access article distributed under the terms and conditions of the Creative Commons Attribution (CC BY) license (<https://creativecommons.org/licenses/by/4.0/>).

## 1. Introduction

Solar energy generated by photovoltaic (PV) modules has received worldwide attention for decades. As most countries, including the U.S., Japan, China, and U.K., have tried to reduce greenhouse gas (GHG) emission, solar energy is becoming even more popular [1]. According to Pehl et al. [2], solar energy generates 6 kg CO<sub>2</sub>-e/MWh, which is a significantly less amount of carbon dioxide equivalent (CO<sub>2</sub>-e) than existing energy sources, such as coal (109 kg CO<sub>2</sub>-e/MWh) and natural gas (78 kg CO<sub>2</sub>-e/MWh). To accelerate the use of solar energy, the Korean government provides a Renewable Energy Certificate (REC) of \$0.11 per kWh, in addition to the System Marginal Price (SMP) of \$0.07 per kWh in 2020 [3–5]. Similarly, the U.S. tries to charge \$0.025 per kg CO<sub>2</sub>-e as GHG emissions [6]. The monetary support has made solar energy competitive, even though its profit is lower than from other existing energy sources.

Due to the government's persistent efforts, the production quantity of solar energy was 1977.1 thousand toe, which is 11.08% of the total production quantity of renewable energy (i.e., 17,837.5 thousand toe) in 2018 in South Korea [7]. In 2020, 16% of 129,191 MW were renewable energy related power plants, and 71% of 20,545 MW were solar energy-based power plants with PV modules [8]. Although this is outstanding progress to reduce the GHG emissions in the future, there was a serious side effect on the environment in South Korea. To be more specific, due to the land shortage problem, small- and mid-size solar power plants have been built on either farmlands or forests. Forests were ravaged and farmlands were destroyed to achieve monetary benefits (i.e., SMP and REC) by producing solar energy [9]. It is contradictory to destroy the environment for the production of electricity via renewable sources.

In fact, the countries (e.g., South Korea, Japan, and China) in Northeast Asia are exposed to a relatively small amount of solar radiation during the day. In particular, South Korea has a daily average global solar radiation of (11–13) MJ/m<sup>2</sup>, and a solar panel can generate electricity for only 6.83 h per day on average [10]. This implies that considerable land has to be used as solar farms (or PV farms). Note that solar farms only generate electricity without cultivating crops. In fact, 425.04 km<sup>2</sup> of land is needed to generate solar energy of 32.2 GW, which is the goal of the Korean government. This is approximately equivalent to 70% of land in Seoul, South Korea [11]. Due to the limited land to build solar power plants, many farms have been transformed into solar power plants (or solar farms) [9]. Regarding solar power efficiency, solar power plants have to be installed in the southwestern region, where large-scale habitable area exists [12]. Since most lands in the southwestern region have been used as farms, it is necessary to adopt the Agrophotovoltaic (APV) system that generates solar power without causing serious harmful impact on the food supply of South Korea. Unlike the existing PV farms, various crops can be cultivated by having a tall pillar to support a solar module in the APV system (see Section 2 for more detail). In 2020, Schindele et al., showed that an APV system with potato production in Germany enables to make annual profit of €10,707/ha and its levelized cost of electricity (LCOE) is 38% higher than that of a PV system [13]. Moreda et al., also showed that an APV system with potato and tomato production in Spain in 2021 can be profitable to a farmer with the minimum internal rates of return (IRRS) of 3.8% [14]. In addition, Kim et al., analyzed profits under six different structures of APV in terms of a shading ratio and a PV panel type to identify an efficient structure of an APV system in South Korea in 2021 [12]. However, there is no study proposing a performance model for development of a profitable APV system.

Thus, the goal of this study is to develop a performance evaluation model for an APV system in South Korea. Two aspects in terms of electricity generation and crop production are considered for the performance evaluation. In particular, estimation models of electricity generation from PV modules have been intensively investigated. Both traditional electricity generation models (i.e., solar radiation-based model and climate-based model) of PV modules and two major machine learning (ML) techniques (i.e., polynomial regression and deep learning) have been considered. Polynomial regression and deep learning are the most popular techniques in the field of ML, and other ML techniques are applications of these techniques [15–17]. Moreover, cost–benefit analysis has been conducted regarding both electricity generation and crop production to provide information about the return on investment to farmers and government agencies. Electricity generation and crop growth data were collected from June to October in 2020 via remote sensors installed in the APV system at Jeollanam-do Agricultural Research and Extension Services in South Korea. As a result, users (i.e., farmers, agronomists, and agricultural engineers) can utilize the proposed model to estimate performance and profit of the APV system, and make a better informed investment decision. Regarding that this study is the first study to develop the performance estimation model for the APV system in terms of both aspects, it will contribute to design and implementation of the system in the world. Furthermore, the proposed model is able to balance energy needs as well as agricultural needs (e.g., food supply) by considering both aspects. This will eventually contribute to the sustainable development of renewable energy systems.

This paper is organized as follows. Section 2 addresses the major components and characteristics of the APV system. In addition, the collected data from the subject APV system in South Korea is analyzed. Section 3 introduces multiple estimation models of the electricity generation of PV modules. Section 4 addresses experiments involving modeling accuracy comparison and cost–benefit analysis. Section 5 presents the findings and concludes the study.

## 2. The Agrophotovoltaic System

The APV system is devised as an alternative to generate electricity from solar modules without causing adverse impact on existing farmlands [12]. The concept of APV was proposed by Getzberger and Zastrow [18], and it has been implemented in multiple countries, including Germany, Japan, China, Italy, the U.S., France, Chile, and South Korea [12,19]. In addition to the continuous production of crops while solar energy is generated, the APV system enhances land productivity, because the soil underneath the solar modules is enabled to keep its moisture, so that soil organic matter can be preserved [20,21]. This implies that the system can also contribute to saving water used for irrigation.

In general, the APV consists of solar modules, supporting structure, a power converter system (pcs), a watt-hour meter, a grid-connected system, and farmland [19,22]. Although its structure is quite similar to a general photovoltaic (PV) plant (or a solar farm), PV modules in the APV system are installed at 2 m (or higher) above the ground [18]. If the farm uses a small tractor (e.g., John Deere 4105) with height of 2.239 m [23], the APV should have clearance height, which results in construction cost increase. Moreover, additional smart farming devices (e.g., solar radiation sensors, temperature and humidity sensors, and soil moisture sensors) are needed to enhance the productivity of the farm. Moreover, until PV farms (or solar power plants) which only maximize electricity productivity, the APV system must consider a shading ratio for crop production. This implies that accurate cost–benefit analysis is needed to identify the profit of the APV system involving a farm, as well as a solar power plant.

In this study, the APV system with an area of 4410 m<sup>2</sup> (63 m × 70 m) at the Jeollanam-do Agricultural Research and Extension Services in Naju-si (35.0161° N, 126.7108° E), Jeollanam-do, South Korea, has been considered to conduct the cost–benefit analysis based on its performance in terms of electricity generation and crop production (see Figure 1a). The subject facility has three areas with monofacial PV modules (i.e., LG405N2W-V5): (1) 787.5 m<sup>2</sup> (31.5 m × 25 m) with shading ratio of 32%, 850.5 m<sup>2</sup> (31.5 m × 27 m) with shading ratio of 25.6%, and 567 m<sup>2</sup> (31.5 m × 18 m) with shading ratio of 21.3%. The height of the supporting structure and pillar cover is (5.42 and 0.81) m, respectively, so that a small tractor (of less than 3 m height) can be used to cultivate crops [12]. To measure the performance of the APV system, multiple sensors involving photosynthetically active radiation (PAR), pyranometer (PYR), temperature and relative humidity (ATMOS14), wind speed and direction (ATMOS22), tipping bucket rain gauge (ECRN-100), and soil moisture, temperature, and electrical conductivity (TEROS 12) have been installed. A farm using the APV system is operated and managed based on the real-time monitoring sensors. This is known as smart farming. Table 1 presents the construction costs of the subject APV system. The lifespan of the subject APV system is expected to be 25 years, which is widely adopted or assumed in the solar power industry, and in the literature [24,25].

**Table 1.** Construction costs of the APV system (edited from Kim et al. [12]).

Data Type	21.3%	25.6%	32%
Number of solar modules (units)	35	56	70
Total construction cost (\$)	17,370.72	27,793.14	34,741.43
Solar module cost (\$)	4961.25	7938.00	9922.50
Structure cost (\$)	8211.81	13,138.90	16,423.63
Electric distribution system cost (\$)	3911.23	6257.97	7822.46
Other costs (\$) <sup>1</sup>	286.42	458.27	572.84
Unit construction cost (\$/module)	496.31	496.31	496.31
Unit construction cost (\$/ha)	153,180.91	163,392.97	220,580.51

<sup>1</sup> The cost includes a building permit fee and a fee for linkage to an existing electric distribution system.

The subject farm is exposed to temperate climate, but the maximum temperature in summer (June–August) is about 30.88 °C on average. Daily average electricity generation per unit area of June, July, August, September, and October are (99.83, 74.95, 97.81, 81.73,

and 88.37) kWh/m<sup>2</sup>/day, respectively. In fact, there is a monsoon season from late June to mid-July, so that the electricity generation quantity of July is lower than other months. Table 2 describes the climate information collected by sensors (e.g., PAR, ATMOS14, ATMOS22, and ECRN-100) installed in the APV system. In order to evaluate performance of the APV system in terms of electricity generation and crop production, this study considers major farming season (June to October) of the subject crops involving sesame, mung bean, red bean, soybean, and corn. Note that PV and APV are inefficient systems to generate electricity in Winter due to low solar radiation and heavy snow. As a result, this study only considers the major farming season which can directly affect farmer's economy.

**Table 2.** Observed climate data.

Month	Solar Radiation (MJ/m <sup>2</sup> )	Surface Temperature High (°C) <sup>1</sup>	Surface Temperature Low (°C) <sup>2</sup>	Precipitation (mm)	Humidity (%)	Windspeed (m/s)
June	3.70	29.40	19.43	12.72	76.93	2.01
July	2.77	27.71	20.92	14.80	84.67	1.94
August	3.62	34.05	24.25	17.83	73.36	2.45
September	3.03	27.74	16.74	7.17	74.11	1.67
October	3.27	24.68	8.73	0.30	56.94	1.67

<sup>1</sup> The highest air temperature; <sup>2</sup> the lowest air temperature.

Figure 1b reveals the daily electricity generation per unit area (kWh/m<sup>2</sup>/day). Under the same climate (see Table 2), the electricity generation amount can vary according to different shading ratios (i.e., (21.3, 25.6, and 32.0)%). This is because the shading ratio increases as the number of installed PV modules per unit area (m<sup>2</sup>) increases. Under the shading ratio condition of 32%, the APV system can have 1.50 times more PV modules than the shading ratio condition of 21.3%. In Figure 1a, the gap between PV modules is different under three shading ratio conditions.

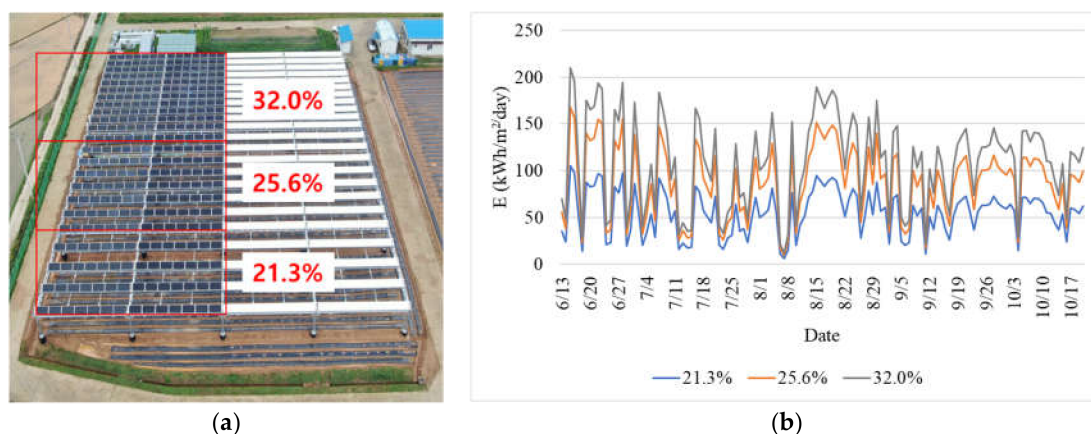


**Figure 1.** Overview of the APV system: (a) APV with three different shading ratios; (b) Electricity generation by the APV system. APV: Agrophotovoltaic.

Unlike electricity generation, the higher shading ratio decreases crop production. Table 3 represents the grain yields of five crops in the APV system [12]. The numbers in parentheses indicate loss (−) or gain (+) in yield, compared to the yield without shading. Among the five crops, only the yield of corn increases under the shading condition of 21.3%. There is minor reduction of the production yields of sesame (*Sesamum indicum*) and soybean (*Glycine max*) at the shading condition of 21.3%. On the other hand, mung bean and red bean are inappropriate crops to be cultivated in the APV system, considering their production yields.

**Table 3.** Harvested grain yields (Mg/ha) of all five crops grown under four different shading levels [12].

Crop Type	Shading Levels (%)			
	0	21.3	25.6	32
Sesame ( <i>Sesamum indicum</i> )	0.96	0.89 (−7%)	0.83 (−14%)	0.45 (−53%)
Mung bean ( <i>Vigna radiata</i> )	1.95	1.54 (−21%)	1.1 (−44%)	1.09 (−44%)
Red bean ( <i>Vigna angularis</i> )	2.35	1.75 (−26%)	1.52 (−35%)	1.47 (−37%)
Corn ( <i>Zea mays</i> )	8.09	8.56 (+6%)	6.4 (−21%)	5.63 (−30%)
Soybean ( <i>Glycine max</i> )	3.64	3.15 (−13%)	2.88 (−21%)	2.54 (−30%)

### 3. Performance Estimation Modeling of an APV System

Although the APV system is a novel concept needing further studies, there are multiple estimation models of PV panels. In this study, to develop a reliable performance estimation model of the APV system in terms of electricity generation and crop production, traditional performance models of electricity generation of PV panels are investigated. Sections 3.1.1 and 3.1.2 will address two major traditional estimation models of PV electricity generation. Sections 3.1.3 and 3.1.4 will enhance existing electricity generation models via ML techniques. Section 3.2 will introduce crop yield estimation models for five crops such as sesame, soybean, red bean, mung bean, and corn.

#### 3.1. Electricity Generation Models of a PV Module

##### 3.1.1. Solar Radiation-Based Model

Equation (1) represents the most popular model to estimate solar energy ( $E$ , kWh) based on three factors, namely daily solar radiation per unit area ( $S$ , kWh/m<sup>2</sup>/day), capacity of a PV module per unit area ( $P_{out}$ , kW/m<sup>2</sup>), and efficiency of electricity generation ( $k$ ) [26,27].

$$E = S \times P_{out} \times k \quad (1)$$

In addition, there is another estimation model (i.e., size-based model) based on the size of PV module ( $A$ , m<sup>2</sup>) and operation hours ( $h$ ) (see Equation (2)).

$$E = A \times P_{out} \times h \quad (2)$$

Although these two models are simple enough to estimate the electricity generation of PV panels, they tend to have low prediction accuracy. Nevertheless, due to their simplicity, they are widely used to estimate the electricity generation of large-scale solar power plants.

##### 3.1.2. Climate-Based Model

To overcome the limitation of the solar radiation-based model, the climate-based model involving air temperature and windspeed was devised [27].

$$E = S \times h(x, y) \times P_{out} \times k \quad (3)$$

where,  $h(x, y)$  is a function of air temperature ( $x$ , °C) and windspeed ( $y$ , m/s).

$$h(x, y) = 742.9 + 176.5x + 3.562y - 13.14x^2 - 0.7466xy - 0.151y^2 \quad (4)$$

In this study, the polynomial regression algorithm (see Section 3.1.3) is applied to enhance the prediction accuracy of Equation (3). Under the given variables (i.e.,  $x$  and  $y$ ), all coefficients have been calibrated with the training data set. Equation (5) represents the revised function of Equation (4):

$$h(x, y) = 0.966 - 2.78 \times 10^{-17}x + 9.44 \times 10^{-16}y + 1.51 \times 10^{-18}x^2 - 3.21 \times 10^{-17}xy - 3.82 \times 10^{-18}y^2 \quad (5)$$

### 3.1.3. Polynomial Regression Model

Polynomial regression (PR) is one of the most popular techniques in the field of machine learning (ML). Unlike the traditional linear regression, it uses any kind of polynomial functions, such as quadratic, cubic, and quartic, so that a non-linear relationship can be accurately captured [28]. Due to its flexibility, PR has also been applied to estimate the electricity generation of PV modules used in the green roof system [29]. In addition, Melit et al. [30] also applied PR to estimate the electricity generation of PV modules, and proved its modeling capability. The major advantage of PR is that it indicates the significance of a predictor via its coefficient value [31]. Equation (6) represents the general PR model [12]:

$$Y = g(X_1, \dots, X_n) = \beta_0 + f_1(X_1) + \dots + f_n(X_n) + \varepsilon, \varepsilon \sim N\left(0, \sum_{j=1}^n \sigma_j^2\right) \quad (6)$$

$$f_j(X_j) = \beta_{j1}(X_j) + \beta_{j2}(X_j^2) + \dots + \beta_{jL}(X_j^L), j = 1, 2, \dots, n \quad (7)$$

where,  $f_j(X_j)$  is a polynomial function on  $X_j$ ,  $\beta_0 = \sum_{j=1}^n \beta_{j0}(X_j^0)$ ,  $X_j^0 = 1$ , and  $\sum_{j=1}^n \beta_{j0}(X_j^0) = \sum_{j=1}^8 \beta_{j0}$ .  $\beta_j$  is a coefficient of  $X_j$ , and  $\beta_0$  is a constant.  $\beta_j$  represents the influence weight of  $X_j$  on response variable  $Y$ . In this study, seven variables are considered: (1)  $X_1$ : daily solar radiation (MJ/m<sup>2</sup>); (2)  $X_2$ : maximum daily temperature (°C); (3)  $X_3$ : minimum daily temperature (°C); (4)  $X_4$ : daily precipitation (mm); (5)  $X_5$ : daily humidity (%); (6)  $X_6$ : daily windspeed (m/s); and (7)  $X_7$ : Shading ratio (%). These variables are identified from existing models (see Sections 3.1.1 and 3.1.2) and literatures [12,19,22].

$$\begin{aligned} E = & -147.38 + 27.16X_1 - 9.61 \times 10^{-2}X_2 + 1.03 \times 10^{-2}X_2^2 - 1.67 \times 10^{-4}X_2^3 \\ & + 2.79 \times 10^{-3}X_3 + 7.39 \times 10^{-3}X_3^2 - 2.93 \times 10^{-4}X_3^3 + 1.59 \times 10^{-3}X_4 \\ & - 3.02 \times 10^{-4}X_4^2 + 1.11 \times 10^{-6}X_4^3 + 5.15 \times 10^{-1}X_5 - 8.23 \times 10^{-3}X_5^2 \\ & + 4.04 \times 10^{-5}X_5^3 - 4.23 \times 10^{-2}X_6 + 507.82X_7 \end{aligned} \quad (8)$$

In Equation (8), most of the variables (except  $X_1$ ,  $X_6$ , and  $X_7$ ) have non-linear relationship with the electricity generation of PV modules. This implies that the traditional linear regression model is inappropriate to estimate the electricity generation.

### 3.1.4. Deep Learning Model

Recently, Deep learning (DL), also known as a multi-layered neural network, has attracted worldwide attention, due to its powerful capability, particularly in image processing. It consists of multiple artificial neurons to process unstructured data, such as images, sounds, and languages [32]. In fact, Barrera et al. [33] utilized the artificial neural network (ANN) to model the solar power generated by a PV module, so that it is also possible to use the DL for electricity generation modeling. Equation (9) represents the  $n^{\text{th}}$  output at layer  $L$  ( $a_n^L$ ) given by multiple hidden layers:

$$a_n^L = \left[ \sigma \left( \sum_m \theta_{nm}^L \left[ \dots \left[ \sigma \left( \sum_j \theta_{kj}^2 \left[ \sigma \left( \sum_i \theta_{ji}^1 x_i + b_j^1 \right) \right] + b_k^2 \right) \right] \dots \right] + b_n^L \right) \right]_n \quad (9)$$

In Equation (9),  $b_n^l$  is bias with  $n$  nodes at  $l$  layer;  $\theta_{nm}^l$  is a weight between  $l$  and  $l - 1$  layers; and  $x_i$  is an input node  $i$ . In this study, the variables identified in Section 3.1.3 are considered for performance comparison between PR and DL models. The deep learning algorithm given by DeepLearning4J library [34] has been used under the computing environment of Intel Core™ i5-8250U CPU @1.60 GHz. The model is developed according to four stages: (1) data preprocessing (or labeling), (2) parameter setting, (3) deep learning modeling, and (4) model evaluation. Figure 2 shows a pseudo code for DL modeling with the DeepLearning4J library.

- 1: INITIALIZE seed, nEpochs, nSamples, batchSize, learningRate.
- 2: SET numbers of input, output, and hidden nodes.
- 3: SELECT XAVIER as a weight initialization method.
- 4: DEFINE the structure of a neural network.
- 5: LOAD train and test data sets.
- 6: RUN the program to develop a DL model via multiple iterations
- 7: RETURN the output.

**Figure 2.** Pseudo code of DL with DeepLearning 4J library.

### 3.2. Crop Yield Estimation Model

This section uses the crop production data under the APV system addressed in Section 2. Table 4 represents the results of analysis of variance (ANOVA). There exist statistical differences between shading ratios, as well as crop types, because the  $p$ -values of both comparisons in crop types and shading ratios are less than  $\alpha = 0.05$ . This means that the crop growth is influenced by the shading ratios, and their impact on crop growth can vary according to crop type. Thus, we need to develop five crop growth models based on the shading ratios.

**Table 4.** Comparison of crop growth with the four shading ratios of (0, 21.3, 25.6, and 32)%.

Source of Variation	Sum of Squares	Degrees of Freedom	Mean Squares	F <sup>1</sup>	$p$ -Value	F Crit <sup>2</sup>
Between shading ratios	104.73	4.00	26.18	99.51	$4.29 \times 10^{-9}$	3.26
Between crop types	4.38	3.00	1.46	5.55	$1.26 \times 10^{-2}$	3.49
Error	3.16	12.00	0.26			
Total	112.28	19.00				

<sup>1</sup> The statistic is given by an F-distribution under the null hypothesis; <sup>2</sup> The critical Type-1 error at  $\alpha = 0.05$ .

In this study, PR addressed in Section 3.1.3 is used, because the experiment only considered four levels of shading ratios, i.e., (0, 21.3, 25.6, and 32)%. Given that the DL requires a big data to achieve statistically reliable results [35], PR is more appropriate for the modeling [31]. Equations (10)–(14) show the developed PR models.

$$G_{sesame} = 0.9579 + 2.6268X_{SR} - 13.006X_{SR}^2 \quad (10)$$

$$G_{mungbean} = 1.9569 - 1.8523X_{SR} - 3.2175X_{SR}^2 \quad (11)$$

$$G_{redbean} = 2.3529 - 3.5503X_{SR} + 2.2487X_{SR}^2 \quad (12)$$

$$G_{corn} = 8.1208 + 15.488X_{SR} - 75.119X_{SR}^2 \quad (13)$$

$$G_{soybean} = 3.6413 - 0.3176X_{SR} - 9.8677X_{SR}^2 \quad (14)$$

In Equations (10)–(14),  $G_{sesame}$ ,  $G_{mungbean}$ ,  $G_{redbean}$ ,  $G_{corn}$ , and  $G_{soybean}$  denote yields of sesame, mung bean, red bean, corn, and soybean, respectively.  $X_{SR}$  is the shading ratio (%) given by the APV system. Note that the yields should be greater than or equal to zero. The  $R^2$  values of the sesame, mung bean, red bean, corn, and soybean models are (97.19, 90.54, 98.31, 83.57, and 99.72)%, respectively. Thus, we can conclude that the five PR models can accurately capture the relationship between crop yields and shading ratios.

## 4. Experiments

### 4.1. Model Comparison

Figure 3 reveals the prediction results of electricity generation of the PV modules. The prediction results shown in Figure 3a,b were estimated by Equations (1) and (2), respectively. Because Equation (2) mainly considers the size and operating hours of the PV module regardless of the strength of solar radiation, it can only capture the variability associated with the capacity of the PV module per unit area ( $P_{out}$ , kW/m<sup>2</sup>) in Figure 3b.

Samples from (1 to 130) were observed from PV modules with a shading ratio of 21.3%; samples from (131 to 260) were observed from PV modules with a shading ratio of 25.6%; and samples from (261 to 390) were observed from PV modules with a shading ratio of 32%. Note that the larger shading ratio has the larger electricity generation capacity per unit area ( $\text{m}^2$ ).  $R^2$  of the size-based model is 22.53%. On the other hand, the solar radiation-based model can consider the intensity of solar radiation during the day, which enables most of the variability to be captured. Its  $R^2$  is 89.39%. To maximize the prediction performance of the estimation model, parameter  $k$  in Equation (1) has been calibrated with a training data set (i.e., 10% of the observed data), and its value is 0.9. Since the electricity generation data was only observed during the summer season, the variability caused by other factors was relatively insignificant in the data set. This results in the high prediction accuracy of Equation (1).

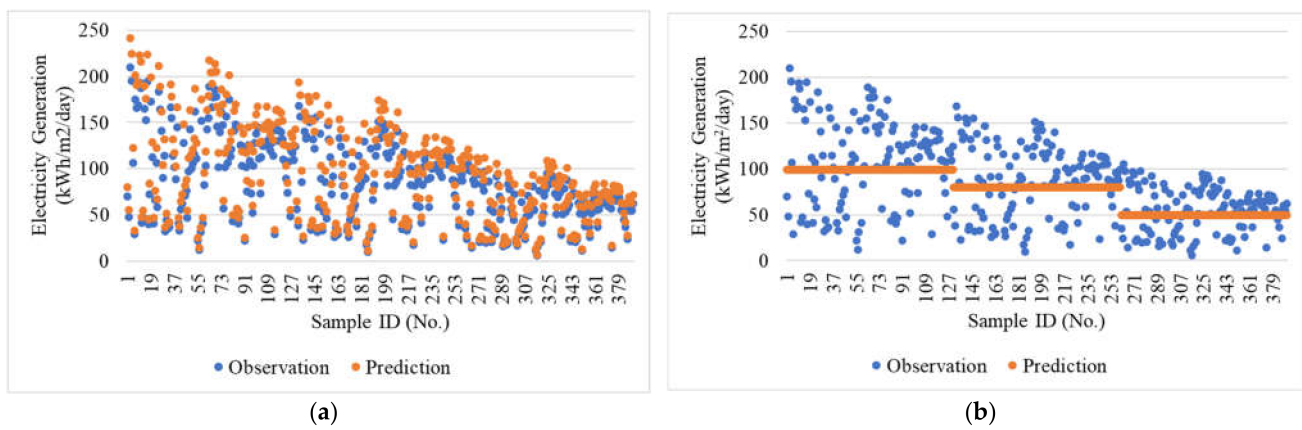


**Figure 3.** Prediction results: (a) solar radiation-based model; (b) size-based model.

Figure 4 shows the prediction results of both climate-based model and polynomial regression model. The climate-based model in Figure 4a uses the updated function of air temperature ( $^{\circ}\text{C}$ ) and windspeed ( $\text{m/s}$ ) shown in Equation (5).  $R^2$  of the model is 94.23%. Regarding the high prediction accuracy of the model, it is better to consider air temperature and windspeed, in addition to the solar radiation used in Equation (1). Similar to the climate-based model, the PR model addressed in Section 3.1.3 has high prediction accuracy (see Figure 4b). The  $R^2$  value of the model is 92.99%. Although the PR model considers more variables, it does not consider the interaction effect between air temperature and windspeed (i.e.,  $xy$ ). That is why its  $R^2$  value is slightly lower than that of the climate-based model. However, because the PR model can consider any multiple variables, it has flexibility.

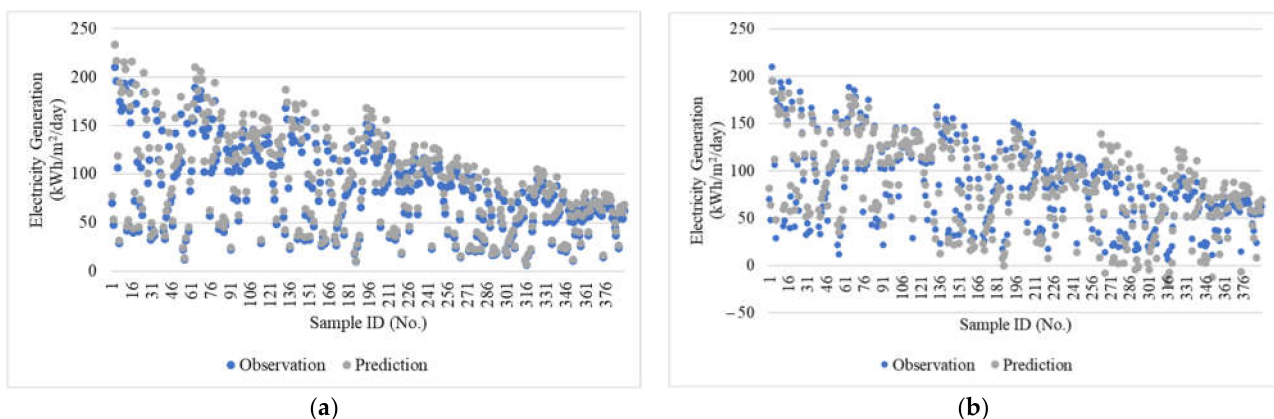


**Figure 4.** Prediction results: (a) climate-based model; (b) polynomial regression model.

Figure 5 shows the prediction result of the DL model. The DL model is developed based on the following parameters: (1) batch size: 100; (2) learning rate: 0.01; (3) loss function: mean square error (MSE); and (4) weight initialization model: Xavier initialization. Figure 5b reveals the prediction accuracy change over various conditions in terms of the number of hidden nodes ( $m$ ). As mentioned in Section 3.1.4, the structure of the DL model can vary under the given parameters. In this study, we change the number of hidden nodes in a neural network layer to identify the best prediction model of the electricity generation. Under the given dataset, the DL model with eight nodes has been identified as the best model; however, other models also provide high prediction accuracy in terms of  $R^2$ . The value range is between (93.60 and 96.42)%. Figure 5a shows the prediction result of the DL model with  $R^2$  of 96.42%. Regarding the results shown in Figures 3 and 4, the DL model can generate the best prediction model in terms of  $R^2$ . Similar to the PR model, it has modeling flexibility, because in the DL model, any variables can be considered.

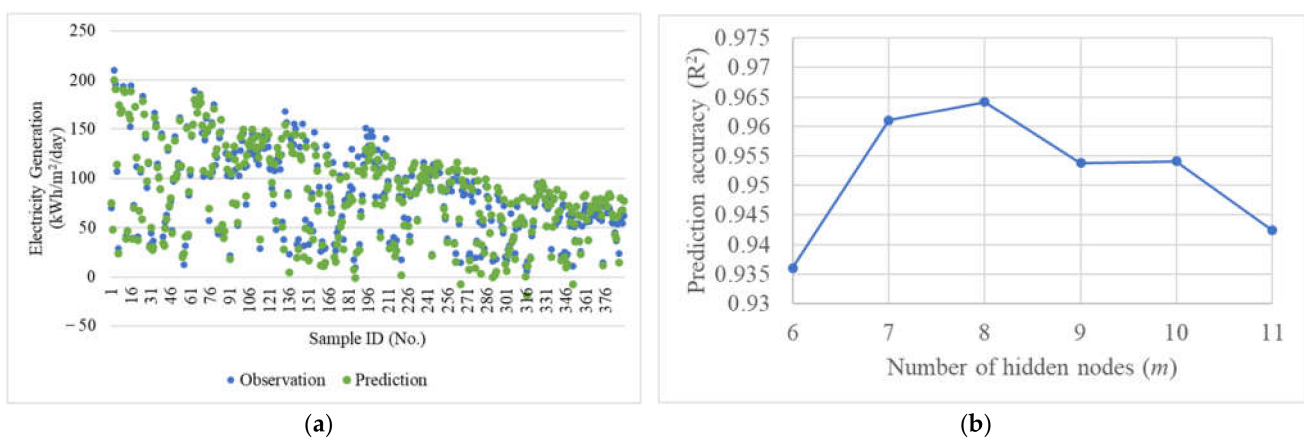


Figure 5. Prediction results: (a) deep learning model with eight hidden nodes; (b) prediction accuracy.

#### 4.2. Cost–Benefit Analysis

Figure 6 reveals the estimated profits given by electricity generation from PV modules in the APV system. The electricity generation on daily average is estimated by the DL model addressed in Section 3.1.4. The System Marginal Price (SMP) and the Renewable Energy Certificate (REC) for solar energy considered in the estimation are \$(0.07 and 0.11)/kWh, respectively [3–5]. Also, we consider the electricity production cost of \$0.15/kWh at the 100 kW solar power plant in South Korea [36]. Based on the cost and sales price information, we assume that the most profitable case is \$0.03/kWh from the electricity generation. In Figure 6, five different unit profits from \$(0.005 to 0.03)/kWh are considered to understand the sensitivity of the unit profit to profit change. In the condition that the unit profit is \$0.005/kWh, the daily profit tends to increase linearly. On the other hand, when the unit profit is \$0.03/kWh, the daily profit increases exponentially as the shading ratio increases.

Figure 7 shows the estimation for the production of the five crops under the APV system. As mentioned in Section 2, corn and sesame have received minor impact of shading ratio on their growth. In particular, the shading ratio of less than 20% can increase crop production of both crops according to the estimated result (see Figure 7a). Unlike corn and sesame, production yields of the other three crops (i.e., mung bean, red bean, and soybean) are almost linearly decreased as the shading ration increases.

Figure 7b shows the profits estimated by PR models in Section 3.2 (see Equations (10)–(14)). The unit profits of sesame, mung bean, red bean, corn, and soybean are \$(5.39, 5.06, 3.67, 1.42, and 2.68)/kg, respectively [12]. Although the unit profit of corn (i.e., \$1.42/kg) is lower than that of the other four crop types, corn has the highest yield among the five crop types, so that its profit (\$/m<sup>2</sup>) is higher than that of any of the other crops. Mung bean and red bean are still profitable, due to their high unit profits (i.e., \$(5.06 and 3.67)/kg).

Soybean has the second highest productivity, so that it is recognized as the second most profitable crop. On the other hand, sesame is the least profitable, due to its cheap unit price of \$2.68/kg, as well as low production yield.

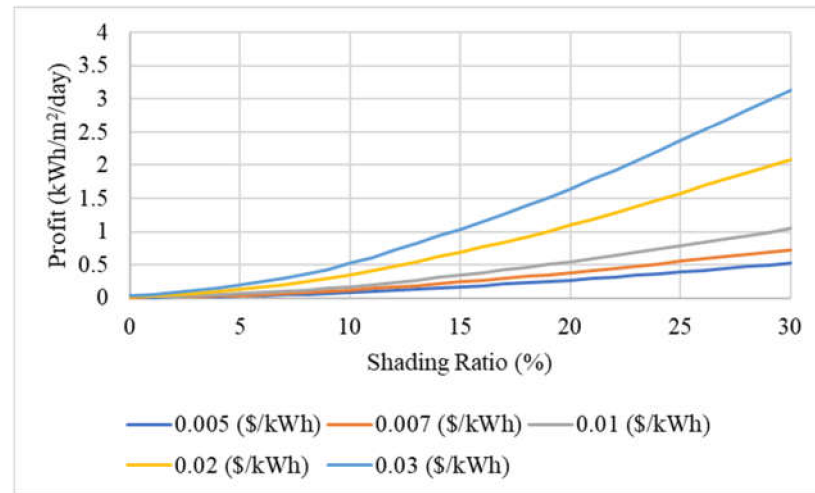


Figure 6. Profit estimation with different shading ratios.

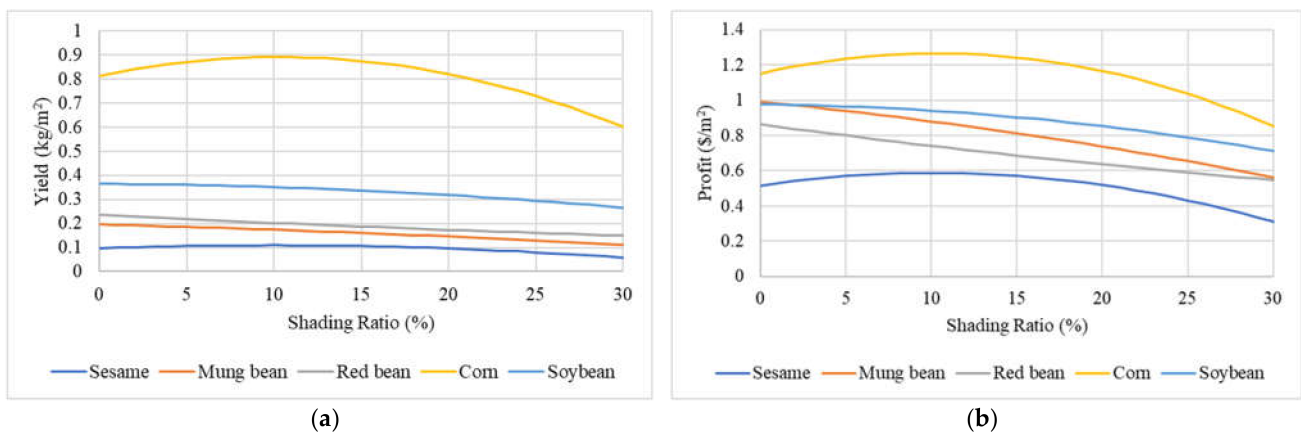
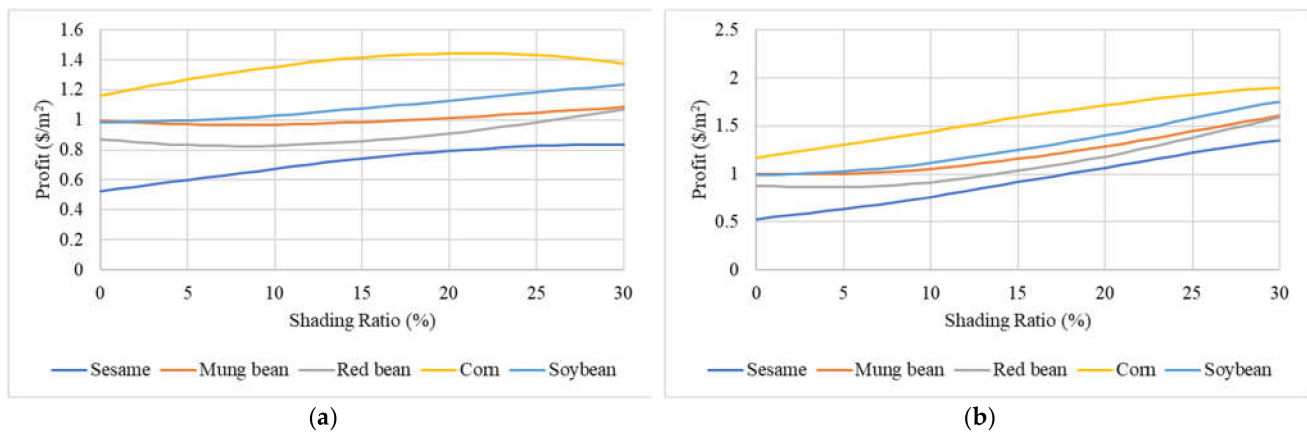


Figure 7. Estimation of crop production with different shading ratios: (a) yields of five crops; (b) profits of five crops.

Figure 8 reveals the total profits of the subject APV system involving electricity generation and crop production. In Figure 8a, the unit electricity profit of \$0.005/kWh is considered to compute the total profit of the APV system. In this case, due to the low rate of the unit electricity profit, the total profit is significantly influenced by crop sales. However, unlike Figure 7a, the shading ratio of 21% is identified as the most profitable shading ratio for corn production. Sesame also shows a similar pattern, and 28% is the most profitable shading ratio. The total profits of the other three crops (i.e., mung bean, red bean, and soybean), which are significantly influenced by shading ratios, have the minimum point around the shading ratio of 10%. Thus, for farms producing these crops, it is better to focus only on either crop production or solar energy production. In fact, the total profit is mainly dependent on electricity generation as the unit electricity profit increases (see Figure 8b). The major advantage of the APV system is that it allows a farmer to increase his or her profit by selling electricity to the government [12]. Also, as shown in Figure 8, a farmer can hedge against REC risk. If REC decreases, the farmer can focus on crop production. If REC increases, s/he can produce more electricity from PV modules.



**Figure 8.** Estimation of the total profit of APV: (a) total profit with \$0.005/kWh; (b) total profit with \$0.01/kWh. APV: Agrophotovoltaic.

## 5. Conclusions

This study has proposed a performance estimation model of the APV system involving solar energy generation and crop production. For accurate performance estimation, both traditional electricity generation models (i.e., the solar radiation-based model and climate-based model) of PV modules and two major machine learning (ML) techniques of PR and DL have been considered. In particular, Deeplearning4j library is used to estimate the electricity generation of the APV system, and the prediction accuracy of the DL model has been compared with that of the other three models. Electricity generation and crop production data was collected via remote sensors installed in the APV system at Jeollanamdo Agricultural Research and Extension Services in South Korea. In the experiments, model performance has been evaluated with the collected data, and economic analysis in terms of cost and profit of the subject APV system has been conducted to provide the investment information to farmers and government agencies.  $R^2$  values of the solar radiation-based model, the climate-based model, the PR model, and the DL model are 89.39%, 94.23%, 92.99%, and 96.42%, respectively. The DL model has the best prediction results, but other models also provide quite accurate prediction results in electricity generation. From these four models, we can conclude that solar radiation and other climate components are significant factors for the electricity generation of the APV system. In addition, PR is used to estimate the production yields of five crops of sesame, mung bean, red bean, corn, and soybean. The  $R^2$  values of the sesame, mung bean, red bean, corn, and soybean models are 97.19%, 90.54%, 98.31%, 83.57%, and 99.72%, respectively. As mentioned in Section 3.1.3, the PR is a flexible technique providing high prediction accuracy. Since the production yields are significantly influenced by the solar radiation, the shading ratio of less than 25% can provide positive impact on production of five crops. Particularly, under the condition of the unit electricity profit of \$0.005/kWh, corn is the most profitable crop with \$1.44/m<sup>2</sup>. As a result, farmers, agronomists, and agricultural engineers are able to accurately estimate the total profit of an APV system via the proposed performance model.

Although the proposed approach successfully estimated the performance of the APV system in terms of crop production and electricity generation, further studies are needed. First, the models should be updated based on field data collected from multiple APV systems in different places to develop a generic performance model. Second, the impact of the APV systems on various crop types in addition to the five crops should be investigated, to maximize farmer's profit.

**Author Contributions:** Conceptualization, S.K. (Sojung Kim); methodology, S.K. (Sojung Kim), S.K. (Sumin Kim); software, S.K. (Sojung Kim); validation, S.K. (Sojung Kim), S.K. (Sumin Kim); resources, S.K. (Sojung Kim); writing—original draft preparation, S.K. (Sojung Kim), S.K. (Sumin Kim); writing—review and editing, S.K. (Sojung Kim), S.K. (Sumin Kim); visualization, S.K. (Sojung Kim),

S.K. (Sumin Kim); project administration, S.K. (Sojung Kim), S.K. (Sumin Kim); funding acquisition, S.K. (Sumin Kim). All authors have read and agreed to the published version of the manuscript.

**Funding:** This work was supported by the National Research Foundation of Korea (NRF) grant funded by the Korea government (MSIT) (No. 2021R1F1A1045855).

**Institutional Review Board Statement:** Not applicable.

**Informed Consent Statement:** Not applicable.

**Data Availability Statement:** Not applicable.

**Conflicts of Interest:** The authors declare that they have no conflict of interest.

## References

- Leggett, J.A.; Lattanzio, R.K.; Ek, C.; Parker, L. *An Overview of Greenhouse Gas (GHG) Control Policies in Various Countries*; Congressional Research Service: Washington, DC, USA, 2009; pp. 1–52.
- Pehl, M.; Arvesen, A.; Humpenöder, F.; Popp, A.; Hertwich, E.G.; Luderer, G. Understanding future emissions from low-carbon power systems by integration of life-cycle assessment and integrated energy modelling. *Nat. Energy* **2017**, *2*, 939–945. [[CrossRef](#)]
- Korea Electric Power Corporation. A Price of the System Marginal Price. Available online: <https://home.kepco.co.kr/kepco/CO/D/E/CODEPP002/list.do> (accessed on 20 April 2021).
- EPSIS. Unit Price of Electricity by Type. Available online: <http://epsis.kpx.or.kr/epsisnew/selectEkmaUpsBftChart.do?menuId=040701> (accessed on 1 April 2021).
- Korea Power Exchange. A Price of the Renewable Energy Certificate. Available online: <https://onerec.kmos.kr/portal/index.do> (accessed on 20 April 2021).
- Congressional Budget Office. Impose a Tax on Emissions of Greenhouse Gases. Available online: <https://www.cbo.gov/budget-options/54821> (accessed on 21 December 2020).
- E-Nara Statistics. Production Status of Renewable Energy. Available online: [https://www.index.go.kr/potal/main/EachDtlPageDetail.do?idx\\_cd=1171](https://www.index.go.kr/potal/main/EachDtlPageDetail.do?idx_cd=1171) (accessed on 31 August 2021).
- Electric Power Statistics Information System. Status of Power Generating Unit in 2020. Available online: <http://epsis.kpx.or.kr/epsisnew/selectEkifBoardList.do?menuId=080402&boardId=040200> (accessed on 31 August 2021).
- Maeil Business News Korea. Ravaged Forests Due to Solar Power Plants. Available online: <https://www.mk.co.kr/news/economy/view/2020/08/845802/> (accessed on 31 August 2021).
- UN Data. Global Solar Radiation. Available online: <https://www.etrans.or.kr/policy/04.php> (accessed on 31 August 2021).
- Yonhap News Agency. 70% of lands in Seoul Are Needed for Solar Power Plants Construction. Available online: <https://www.yna.co.kr/view/AKR20201006172900001> (accessed on 31 August 2021).
- Kim, S.; Kim, S.; Yoon, C.Y. An Efficient Structure of an Agrophotovoltaic System in a Temperate Climate Region. *Agronomy* **2021**, *11*, 1584. [[CrossRef](#)]
- Schindele, S.; Trommsdorff, M.; Schlaak, A.; Obergfell, T.; Bopp, G.; Reise, C.; Braun, C.; Weselek, A.; Bauerle, A.; Högy, P.; et al. Implementation of agrophotovoltaics: Techno-economic analysis of the price-performance ratio and its policy implications. *Appl. Energy* **2020**, *265*, 114737. [[CrossRef](#)]
- Moreda, G.P.; Muñoz-García, M.A.; Alonso-García, M.C.; Hernández-Callejo, L. Techno-Economic Viability of Agro-Photovoltaic Irrigated Arable Lands in the EU-Med Region: A Case-Study in Southwestern Spain. *Agronomy* **2021**, *11*, 593. [[CrossRef](#)]
- Cheng, X.; Khomtchouk, B.; Matloff, N.; Mohanty, P. Polynomial regression as an alternative to neural nets. *arXiv* **2018**, arXiv:1806.06850.
- Hwang, J.; Lee, J.; Lee, K.S. A deep learning-based method for grip strength prediction: Comparison of multilayer perceptron and polynomial regression approaches. *PLoS ONE* **2021**, *16*, e0246870. [[CrossRef](#)] [[PubMed](#)]
- Bamisile, O.; Oluwasanmi, A.; Ejiyi, C.; Yimen, N.; Obiora, S.; Huang, Q. Comparison of machine learning and deep learning algorithms for hourly global/diffuse solar radiation predictions. *Int. J. Energy Res.* **2021**. [[CrossRef](#)]
- Goetzberger, A.; Zastrow, A. On the coexistence of solar-energy conversion and plant cultivation. *Int. J. Sol. Energy* **1982**, *1*, 55–69. [[CrossRef](#)]
- Weselek, A.; Ehmann, A.; Zikeli, S.; Lewandowski, I.; Schindele, S.; Högy, P. Agrophotovoltaic systems: Applications, challenges, and opportunities. A review. *Agron. Sustain. Dev.* **2019**, *39*, 1–20. [[CrossRef](#)]
- Dupraz, C.; Marrou, H.; Talbot, G.; Dufour, L.; Nogier, A.; Ferard, Y. Combining solar photovoltaic panels and food crops for optimising land use: Towards new agrivoltaic schemes. *Renew. Energy* **2011**, *36*, 2725–2732. [[CrossRef](#)]
- Hassanpour Adeg, E.; Selker, J.S.; Higgins, C.W. Remarkable agrivoltaic influence on soil moisture, micrometeorology and water-use efficiency. *PLoS ONE* **2018**, *13*, e0203256. [[CrossRef](#)] [[PubMed](#)]
- Zohdi, T.I. A digital-twin and machine-learning framework for the design of multiobjective agrophotovoltaic solar farms. *Comput. Mech.* **2021**, 1–14.
- John Deere. Compact Tractors : 22.4–65.9 HP. Available online: <https://www.deere.com/en/tractors/compact-tractors/> (accessed on 8 September 2021).

24. Kannan, R.; Leong, K.C.; Osman, R.; Ho, H.K.; Tso, C.P. Life cycle assessment study of solar PV systems: An example of a 2.7 kWp distributed solar PV system in Singapore. *Sol. Energy* **2006**, *80*, 555–563. [[CrossRef](#)]
25. LG. LG Solar Module Limited Warranty. Available online: [https://www.lg.com/us/business/download/resources/BT00002151/BT00002151\\_2573.pdf](https://www.lg.com/us/business/download/resources/BT00002151/BT00002151_2573.pdf) (accessed on 8 September 2021).
26. Ayvazođluyüksel, Ö.; Filik, Ü.B. Estimation methods of global solar radiation, cell temperature and solar power forecasting: A review and case study in Eskişehir. *Renew. Sustain. Energy Rev.* **2018**, *91*, 639–653. [[CrossRef](#)]
27. Cha, W.C.; Park, J.H.; Cho, U.R.; Kim, J.C. A study on solar power generation efficiency empirical analysis according to temperature and wind speed. *Trans. Korean Inst. Electr. Eng.* **2015**, *64*, 1–6.
28. Kim, S.; Meng, C.; Son, Y.J. Simulation-based machine shop operations scheduling system for energy cost reduction. *Simul. Model. Pract. Theory* **2017**, *77*, 68–83. [[CrossRef](#)]
29. Kim, S.; Aydın, B.; Kim, S. Simulation Modeling of a Photovoltaic-Green Roof System for Energy Cost Reduction of a Building: Texas Case Study. *Energies* **2021**, *14*, 5443. [[CrossRef](#)]
30. Mellit, A.; Sađlam, S.; Kalogirou, S.A. Artificial neural network-based model for estimating the produced power of a photovoltaic module. *Renew. Energy* **2013**, *60*, 71–78. [[CrossRef](#)]
31. Kim, S.; Kim, S.; Cho, J.; Park, S.; Jarrín Perez, F.X.; Kiniry, J.R. Simulated biomass, climate change impacts, and nitrogen management to achieve switchgrass biofuel production at diverse sites in US. *Agronomy* **2020**, *10*, 503. [[CrossRef](#)]
32. Chang, C.W.; Lee, H.W.; Liu, C.H. A review of artificial intelligence algorithms used for smart machine tools. *Inventions* **2018**, *3*, 41. [[CrossRef](#)]
33. Barrera, J.M.; Reina, A.; Maté, A.; Trujillo, J.C. Solar Energy Prediction Model Based on Artificial Neural Networks and Open Data. *Sustainability* **2020**, *12*, 6915. [[CrossRef](#)]
34. DL4J. Deep Learning for Java. Available online: <https://deeplearning4j.org/> (accessed on 8 September 2021).
35. LeCun, Y.; Bengio, Y.; Hinton, G. Deep learning. *Nature* **2015**, *521*, 436–444. [[CrossRef](#)] [[PubMed](#)]
36. Lee, K.; Kim, D. Estimation of Levelized Cost of Electricity for Supply of Renewable Energy. Korea Energy Economics Institute 2020. Available online: <https://www.keei.re.kr/main.nsf/index.html> (accessed on 8 September 2021).